Environ. Eng. Res. Vol. 10, No. 4, pp. 165~173, 2005
Korean Society of Environmental Engineers

SYNTHESIS OF NANO-SIZED IRON FOR REDUCTIVE DECHLORINATION.

1. Comparison of Aerobic vs. Anaeriobic Synthesis and Characterization of Nanoparticles

Hocheol Song[*], Elizabeth R. Carraway[*], and Young-Hun Kim[,†]**

[*]Department of Environmental Engineering and Science, Clemson University
342 Computer Court, Anderson, SC 29625

[**]Department of Environmental Engineering, College of Engineering, Andong National University, Andong, KyungPook 760-749, Korea

(received February 2005, accepted July 2005)

Abstract : Nano-sized iron particles were synthesized by reduction of Fe^{3+} in aqueous solution under two reaction conditions, aerobic and anaerobic, and the reactivity of iron was tested by reaction with trichloroethene (TCE) using a batch system. Results showed that iron produced under anoxic condition for both synthesis and drying steps gave rise to iron with higher reduction reactivity, indicating the presence of oxygen is not favorable for production of nano-sized iron deemed to accomplish reactivity enhancement from particle sized reduction. Nano-sized iron sample obtained from the anoxic synthesis condition was further characterized using various instrumental measurements to identify particle morphology, composition, surface area, and particle size distribution. The scanning electron microscopic (SEM) image showed that synthesized particles were uniform, spherical particles (< 100 nm), and aggregated into various chain structures. The effects of other synthesis conditions such as solution pH, initial Fe^{3+} concentration, and reductant injection rate on the reactivity of nano-sized iron, along with standardization of the synthesis protocol, are presented in the companion paper.

Key Words : Zero-valent metals, Nano-scale iron, Synthesis condition, Anoxic, Reduction

INTRODUCTION

Synthesis of nano-sized metals is a relatively new area in solid state chemistry. Due to their small size and structure, nano-sized metals exhibit novel physical, chemical, and biological properties which are largely different from the bulk solid state.[1] The unique properties of nano-sized metals are derived in part from the fact that their properties lie somewhere between those of the bulk and molecular state.[2] For such reasons, nano-sized metals are very attractive materials for many environmental applications in pollution prevention materials, pollution sensing and detection, and chemical catalysts or reactants for remediation purposes.[3]

The synthesis of nano-sized metals falls into two broad categories: (1) precipitation from a salt solution, and (2) condensation from the vapor phase. These include precipitation from inverse micelle solutions, precipitation from aqueous solutions, laser ablation, spray pyrolysis, gas condensation using either an evaporative source or chemical precursor, and electrochemical deposition in a template membrane. The

† Corresponding author
E-mail: youngkim@andong.ac.kr
Tel: +82-054-820-5818, Fax: +82-054-820-6187

major differences in each of these techniques are particle size, size distribution, morphology, purity, and the degree of aggregation of the particles from each synthesis.[4] While some of these processes, such as precipitation from a solution, can produce very small individual particles (< 10 nm), others, such as condensation from vapor evaporation, usually produce grains in the 20-50 nm size range.[4]

Among the particle synthesis methods, precipitation from aqueous solution is probably the most feasible and widely used method to produce nano-sized metals for environmental applications. This method involves reduction of metal salts in an aqueous solution with a bulk reductant to precipitate the desired metal particles, and has been frequently used to synthesize metal alloys with certain compositional specification because the formation of desired multi-components particles can be achieved simply by using a mixture of metal salts. An important characteristic of particles prepared by this method is an amorphous structure, which gives them a higher reactivity when used as chemical catalysts.[5] In the synthesis, sodium- or lithium borohydride is frequently used as the reductant in the synthesis and the reaction proceeds quite rapidly because of the sufficiently low reduction potential of borohydride ion ($E_1 = -1.31V$).[6]

The application of nano-sized iron synthesized by precipitation method to the destruction of organic contaminants was first reported by Wang and Zhang[7] who prepared nano-sized iron and palladium coated nano-sized iron, and used them as reductants for TCE and a PCBs mixture. Their results indicated that both nano-sized iron particles showed enhanced reactivity compared to commercial grade micro-sized iron. Following the pioneering work of Wang and Zhang, a number of researchers have studied nano-sized iron and applied it to different types of contaminants including chlorinated ethenes,[8,9,11] chlorinated methanes,[10,12] chlorinated benzenes,[8,13] chromium,[14,15] lead,[14,15] and nitrate.[16] The results from these studies were promising in that this new approach supplies not only substantially improved contaminant degradation, but also curtailed production of undesirable byproducts from the reduction.

However, most of the studies reported to date involved precipitation of nano-sized iron in solution open to ambient atmosphere so that oxygen was not excluded in the reaction. When reacted to Fe^{3+}, oxygen readily forms various iron oxide minerals such as hematite (α-Fe_2O_3), maghemite (γ-Fe_2O_3), and magnetite (Fe_3O_4). These minerals will either precipitate out as discrete particles or co-precipitate with iron to form surface oxides. Although the role of surface oxides as a semi-conductor to mediate electron transfer has been previously reported,[17] it is generally assumed that the presence of surface oxides would reduce the reaction rate by acting as a physical barrier that inhibits electron transfer from iron to substrates. Therefore, excluding oxygen during the synthesis of iron may offer a better protocol to obtain iron with superior reactivity for use in destruction of organic contaminants through chemical reduction.

Current study is focusing on the improvement of the activity of the metal surfaces which is usually achieved by bimetallic combination in previous studies.[18]

The objectives of this study are to demonstrate synthesis of nano-sized zero valent iron particles using borohydride reduction of Fe^{3+} in aqueous system, to investigate the impact of oxygen on the reactivity of the final product, and to characterize the iron synthesized under aerobic and anaerobic conditions employed in this study.

EXPERIMENTS AND MATERIALS

Materials

All chemicals were used as received. Chemicals used in this study were trichloehtylene (99.9%, HPLC grade, Sigma), methanol (99.9%, HPLC grade, Burdick & Jackson), pentane (99.9%, GC grade, Burdick & Jackson), toluene (99.9%, HPLC grade, Burdick & Jackson), acetone (99.9%, HPLC grade, Burdick & Jackson), $FeCl_3 \cdot 6H_2O$ (Aldrich) and $NaBH_4$

(Aldrich). Stock solutions of target compounds were prepared by dissolving an appropriate amount of compounds into methanol. Deionized water purified by a Milli-Q water system ($\approx$18 MΩ · cm) (water, hereafter) was purged at least 12 hours to remove O_2 with high purity N_2 that was further purified using an oxygen trap coupled with oxygen indicator. For quality assurance, complete deoxygenation of water was verified by adding a reduced redox indicator solution (resazurin) into the water in an anaerobic chamber (Coy Co.). A pink color was developed when O_2 was present, and the water prepared by the method employed did not indicate the presence of O_2. The atmosphere of the anaerobic chamber was monitored for O_2 contamination at all times by placing vials containing the indicator solution in the chamber.

Synthesis of Nano-sized Iron

Nano-sized iron was synthesized by chemical reduction of iron salt ($FeCl_3 \cdot 6H_2O$) by a strong reductant ($NaBH_4$) as indicated by the following reaction:

$$Fe(H_2O)_6^{3+} + 3BH_4^- + 3H_2O \rightarrow Fe^0 \downarrow + 3B(OH)_3 + 10.5H_2 \quad (1)$$

A Fe^{3+} (0.4 M) solution was prepared by dissolving $FeCl_3 \cdot 6H_2O$ in water. The $NaBH_4$ (1.2 M) solution was also prepared in the anaerobic chamber. Outside the chamber, the $NaBH_4$ solution was added dropwise to the ferric solution while the mixture was vigorously stirred by a mechanical stirrer or a magnetic stirrer under air or N_2 atmosphere. As the reaction continued, a black precipitate started to form. Upon the completion of reaction, the metal particles were filtered with a microfiber filter and washed with water three times (1L H_2O/1g Fe^0), followed by acetone washing to expedite drying of the particles. The iron was dried under air or N_2 atmosphere and used for the reactivity test against TCE. The iron synthesis protocol is explained in more detail in the companion paper.[19]

Reactivity Tests

TCE reduction experiments were carried out using 125 mL amber glass bottles (VWR). To each pre-washed bottle, a known mass of synthesized iron was added in the anaerobic chamber, followed by charging with water leaving 1 mL of headspace. Headspace was allowed to keep the bottle from bursting due to pressure buildup from hydrogen gas evolution. The bottles were sealed with Teflon® lined silicon septa (VWR) and Mininert® caps (VICI). Bottles were then removed from the chamber and the reaction was initiated by spiking a known volume (typically 10 to 100 μL) of methanolic stock solution of TCE through the sampling port of the Mininert® cap using an gas-tight micro-syringe (Hamilton). Control bottles were prepared in the same manner as reaction bottles except addition of iron metal was omitted. Reaction bottles were then mixed in an end-over-end fashion at 40 rpm and at room temperature (23$\pm$1°C) using a rotator (Cole-Parmer). At selected intervals, a 0.5 mL sample was withdrawn using a 1 mL air-tight syringe (Hamilton) from the bottle through the sampling port, followed by injection of an equal volume of water to maintain constant headspace. Unless otherwise stated, all the reactors were prepared in duplicate.

Analytical Methods

A 0.5 mL aliquot withdrawn from the reactor was transferred immediately to a crimp-capped 2 mL GC autosampler vial, which contained 0.5 mL pentane with 5 mg/L toluene as an internal standard. Due to the high volatility of pentane and TCE, the crimp cap was replaced with a new one after the introduction of the sample solution to minimize the losses of pentane and TCE during the extraction of target compounds. The contents of the vial were then mixed using a votex mixer (Fisher Scientific) for 3 minutes and further mixed at 200 rpm on an environmental shaker (New Brunswick Scientific) for 30 minutes. After extraction, 0.2 mL of the pentane layer was transferred to a GC auto-

sampler vial with a 0.3 mL glass insert for GC analysis. TCE was identified and quantified with a HP G1800A GCD with an electron ionization mass spectrometer detector equipped with a DB-VRX column (60 m length, 0.25 mm diameter, 1.8 μm film thickness) (J&W Scientific). The sample (2 μL) was injected in split mode with a split ratio of 30:1. The carrier gas was ultra high purity grade helium and the flow rate was 1 mL/min. The oven temperature was held at 70°C for 8 minutes, increased at 20°C/min to 160°C and held for 2.5 minutes. The injector and detector temperatures were 230°C and 300°C, respectively. For data acquisition, the selected ion monitoring (SIM) mode was used to increase detection sensitivity. In the SIM mode, only two selected ions from the mass spectrum, one as qualifier and one as quantifier, are monitored by the detector, which allows more ion scans in a given time and thus increases detector sensitivity for analytes. The detection limit for TCE as determined by an U.S.EPA protocol[20] was 0.026 mg/L.

Characterization of Nano-sized Iron

Microscopic images of nano-sized iron were obtained through a Hitachi HD-2000 scanning transmission microscopy (STEM) and a Hitachi S-4700 field emission scanning electron microscopy (FESEM). Surface elemental analysis was conducted with energy-dispersive X-ray spectrometer (EDS). The composition of particle was determined using a Perkin Elmer-Sciex Elan 9000 inductively coupled plasma spectrophotometer (ICP). The surface area of iron particles was measured by the Kr adsorption BET method using a Micromeritics ASAP 2010 surface area analyzer. The particle size and distribution were determined using a particle size analyzer Malvern Mastersizer S.

RESULTS AND DISCUSSION

Comparison of Reactivity of Nano-sized Iron

Figure 1 shows the reduction of TCE by nano-sized iron synthesized under two atmospheric conditions during the particle formation reaction. For both iron samples, the precipitated iron was washed and dried under N_2 atmosphere. As the figure reveals, reduction of TCE proceeded at faster reaction rate for iron precipitated under N_2, removing 0.05 mM of TCE in 220 hrs of reaction time. Of note is that the TCE concentration started to decrease after initial lag period ($\approx$30 hrs) for both iron samples. The initial lag period observed is probably the time required for dissolution of unreactive iron (hydr)oxides, which may have precipitated on the surface of iron during the synthesis. In the synthesis of iron under the conditions of this study, the solution pH started out around 1.2 and increased to around 8.5 at the end of $NaBH_4$ addition. Therefore, Fe^{3+}, if not been reduced to Fe^0, is more than likely to precipitate out as (hydr)oxide minerals (e.g. $Fe(OH)_3$) in the moderate pH region because of very low solubility of Fe^{3+} in that region. Once formed, iron (hydr)oxides are likely to deposit on the iron surface since iron (hydr)oxide colloids would be destabilized through electrical double layer compression caused by overwhelmingly

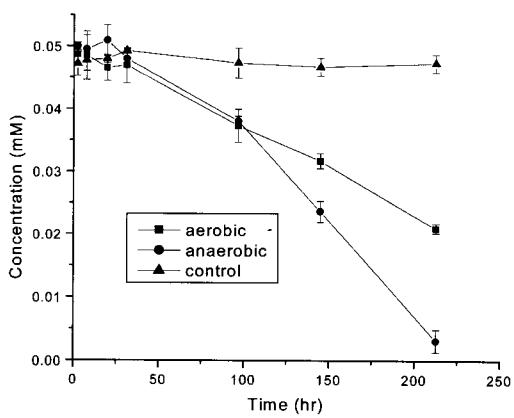

Figure 1. Reduction of TCE by nano-sized iron synthesized under two atmospheric conditions during the particle formation reaction. Iron dose of 0.05 g was used in 124 mL solution. Error bars represent the corresponding concentration ranges. Lines connect points and are not first order fits.

high concentrations of electrolytes (Na^+, Cl^-)[21], and stick to preexisting iron particles. No efforts were made to remove those iron (hydr)oxides for iron samples prior to reduction experiments.

The slower TCE reduction observed for the iron synthesized under aerobic condition suggests other mineral phases may have been formed in the presence of oxygen during the synthesis, along with Fe^0. Iron oxides such as hematite and maghemite are known to inhibit electron transfer and catalytic hydrogenation; two main mechanisms of reduction of chlorinated compounds by iron. In addition, another possibility for the lower reactivity of iron synthesized in the presence of oxygen is the immediate oxidation of iron following the formation. Considering the vigorous mixing provided during the synthesis, the rate of oxygen transfer into water is expected to be sufficiently high enough to support oxidation reactions

The reduction of TCE by nano-sized iron prepared under different drying conditions is shown in Figure 2. For both iron samples, particle formation reaction and washing were carried out under N_2 atmosphere. The result indicates that iron dried under air showed no appreciable sign of TCE reduction, while iron dried under N_2 completely removed TCE over the duration of the experiment. Visual inspection of the iron samples after drying showed the air-dried iron was completely passivated into reddish colored iron oxides. On the contrary, N_2-dried iron remained black, indicating iron remained intact during the drying process. Also, N_2-dried iron underwent strong exothermic oxidation reaction when exposed to air.

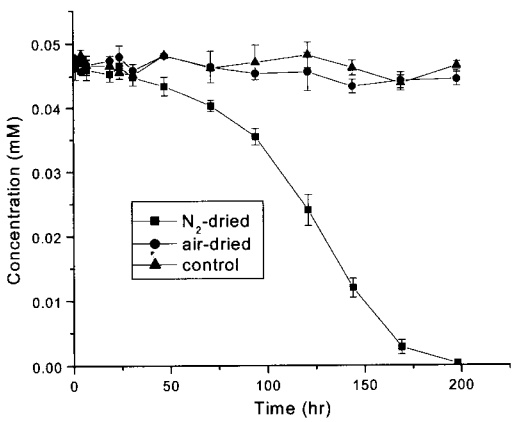

Figure 2. Reduction of TCE by nano-sized iron dried under two atmospheric conditions. Iron dose of 0.05 g was used in 124 mL solution. Error bars represent the corresponding concentration ranges. Lines connect points and are not first order fits.

Characterization of Nano-sized Iron

The nano-sized iron characterized in this study was the one for which all synthesis procedures including chemical solution preparation, reaction, washing and drying were carried out under anaerobic condition to prevent exposure of iron to oxygen during the synthesis. Also, for better characterization of the properties only pertaining to the iron itself, an attempt was made to remove surface impurities (i.e. iron (hydr)oxides) by performing acid washing of iron particles. Figure 3 shows microscopic images of nano-sized iron measured by FESEM. The images were obtained to identify the size and size distribution of the iron particles synthesized. As the microscopic images reveal, particles are uniform in size (mostly <100nm) and shape. The particle size obtained in this study is consistent with other studies employing borohydride reduction for iron synthesis.[11,13,15] Agglomeration of particles is apparent, presumably due to the magnetic interactions between the iron particles.[22] Other microscopic images for nano-sized iron measured with STEM are shown in Figure 4. STEM has better resolution at high magnifications (> × 100 K) than FESEM, and can be operated in scanning electron microscopic (SEM) and transmission electron microscopic (TEM) modes at the same time.[23] As shown in Figure 4(a), STEM provides better resolution of the image and more detailed information on surface morphology. Iron particles have uneven surface textures with protuberances developed on the surface. Since nano-sized iron can be easily oxidized in air and exposure of iron to air was unavoidable during

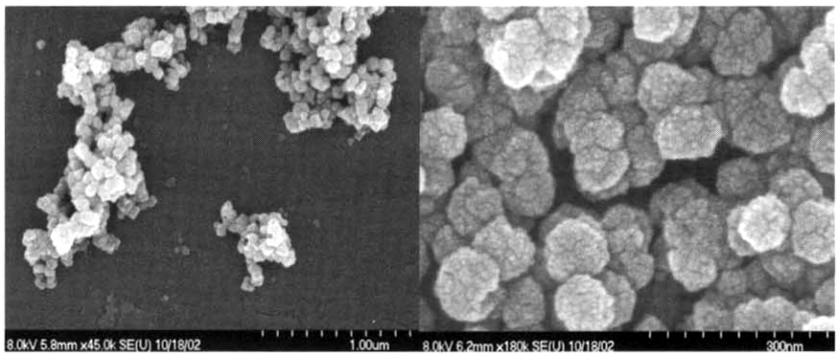

Figure 3. Field emission scanning electron microscopic (FESEM) images of nano-sized iron.

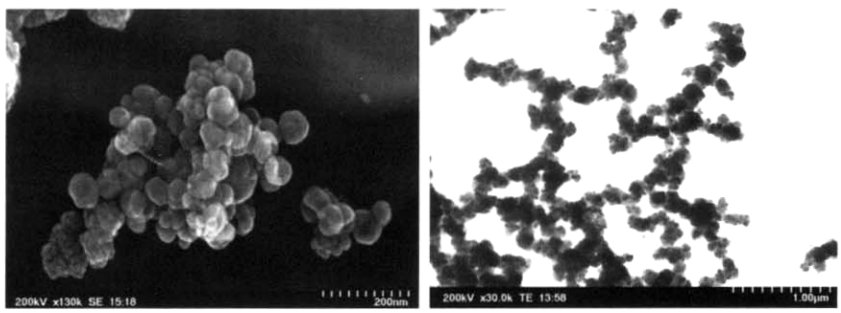

Figure 4. Scanning transmission electron microscopic (STEM) images of nano sized iron measured in (a) SEM and (b) TEM mode.

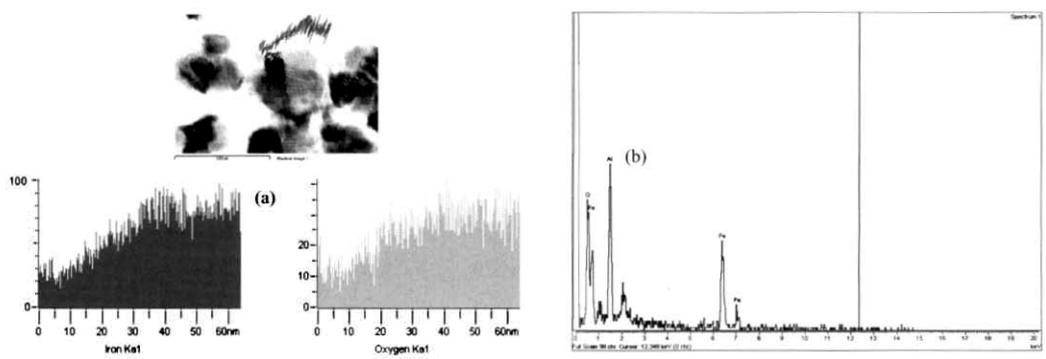

Figure 5. Surface composition of nano-sized iron. (a) Surface elemental mapping of nano- sized iron measured with STEM. (b) Energy dispersive X-ray spectroscopic pattern of nano-sized iron measured by FESEM.

the measurement, surface oxidation might have occurred after the iron was removed from the anaerobic chamber for the measurement. Therefore, it is not clear whether those protuberances are the physical characteristic of iron as synthesized or the products of surface oxidation after exposing to air. The presence of oxygen on the iron surface was confirmed from the elemental mapping obtained with STEM and EDS spectrum with FESEM (Figure 5(a),(b)). The aluminum peaks observed in the EDS spectrum obtained by FESEM are the signals from the Al-sample stub that was used to place iron samples on the top of the sample stub.

ICP data showed that the iron and boron content of the particles were 92.0±0.4% and 7.0±0.4%, respectively, for 6 samples synthesized under the same conditions. No other elements were detected by ICP analyses except for the trace metals contained in the HCl that was used for digestion of the iron samples. Schrick et al. reported 83% iron and 4% boron content for the nano-sized iron synthesized using borohydride reduction.[11] Lower iron content observed in their study is probably due to higher oxygen content in their iron since the iron was synthesized in aerobic conditions in their study so that oxidation of iron might have occurred during the synthesis. Further, pH was raised to around 7 before adding $NaBH_4$ in their synthesis, and this might have led to precipitation of iron (hydr)oxides minerals even before the reduction of Fe^{3+} was initiated. An oxygen content of 44% measured for their iron from X-ray photoelectron spectroscopy (XPS) analysis indicated the presence of (hydr)oxides.

The particle size distribution profile obtained from the particle size analyzer is shown in Figure 6. The overall sizes of particles in the figure are approximately 10 to 20 times bigger than microscopic images. However, as seen from the microscopic images in Figures 4 and 5, particles are agglomerated forming various shaped islands with different sizes. Since the measurement of particle size is based on light blockage by the sample particles and collection of undisturbed light signals on the detector, it gives information on the size of agglomerated particles unless particles are forced to separate. Therefore, the particle size distribution in Figure 6 depicts the size of agglomerated iron particles.

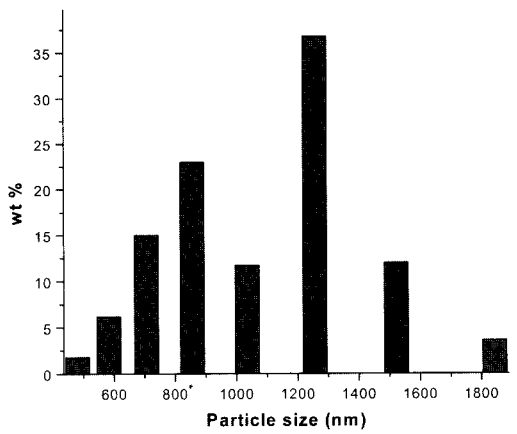

Figure 6. Particle size distribution of nano-sized iron.

The average specific surface area using BET gas adsorption isotherm with Kr gas in the relative pressure range between 0.06 atm and 0.21 atm gave 27.88±1.69 m^2/g for five iron samples. This value is in good agreement with other studies employing borohydride reduction for nano-sized iron synthesis, which ranges from 18 to 35 m^2/g.[7,12,15]

CONCLUSIONS

Synthesis of nano-sized iron through reductive precipitation of Fe^{3+} by $NaBH_4$ was studied. This wet reduction technique was investigated for its wide use and economic viability for environmental application and the following conclusions were drawn.

1. The anoxic condition was favored in the reductive precipitation step for producing nano-sized iron with greater reactivity to TCE.
2. Drying the particle under N_2 atmosphere preserved the reactivity of iron, while air-drying resulted in complete passivation of iron.
3. Nano-sized iron synthesized under the anaerobic conditions of this study was spherical, uniform (<100 nm), and aggregated into various chain structures.
4. The elemental composition of particle was 93% Fe : 7% B. The specific surface area was 27.88±1.69 m^2/g, which is in good agreement with other studies employing similar method of iron synthesis.

REFERENCES

1. Ozin, G. A., "Nanochemistry-Synthesis in diminishing dimensions," *Adv. Mat.*, **4**(10), 612-649 (1992).

2. Aiken, J. D. and Finke, R. G., "A review of modern transition-metal nanoclusters: Their synthesis, characterization, and applications in catalysis," *J. of Mol. Cat.s A-Chem.*, **145** (1-2), 1-44 (1999).
3. Masciangioli, T. and Zhang, W. X., "Environmental technologies at the nanoscale," *Environ. Sci. & Tech.*, **37**(5), 102A-108A (2003).
4. Kear, B. H. and Skandan, G., "Overview: Status and current developments in nanomaterials," *Int. J. of Powder Metallurgy*, **35**(7), 35-37 (1999).
5. Forster, G. D., Barquin, L. F., Bilsborrow, R. L., Pankhurst, Q. A., Parkin, I. P., and Steer, W. A., "Sodium borohydride reduction of aqueous iron-zirconium solutions: Chemical routes to amorphous and nanocrystalline Fe-Zr-B alloys," *J. of Mat. Chem.*, **9**(10), 2537-2544 (1999).
6. Shen, J., Li, Z., Yan, Q., and Chen, Y., "Reactions of bivalent metal ions with borohydride in aqueous solution for preparation of ultrafine amorphous alloy paticles," *J. of Phy. Chem.*, **97**, 8504-8511 (1993).
7. Wang, C. B. and Zhang, W. X., "Synthesizing nanoscale iron particles for rapid and complete dechlorination of TCE and PCBs," *Environ. Sci. & Tech.*, **31**(7), 2154-2156 (1997).
8. Zhang, W. X., Wang, C. B., and Lien, H. L., "Treatment of chlorinated organic contaminants with nanoscale bimetallic particles," *Cat. Today*, **40**(4), 387-395 (1998).
9. Lien, H. L. and Zhang, W. X., "Nanoscale iron particles for complete reduction of chlorinated ethenes," *Col. and Surf. A-Physicochemical and Engineering Aspects*, **191** (1-2), 97-105 (2001).
10. Lien, H. L. and Zhang, W. X., "Transformation of chlorinated methanes by nanoscale iron particles," *J. of Environ. Eng.-ASCE*, **125**(11), 1042-1047 (1999).
11. Schrick, B., Blough, J. L., Jones, A. D., and Mallouk, T. E., "Hydrodechlorination of trichloroethylene to hydrocarbons using bimetallic nickel-iron nanoparticles," *Chem. of Mat.*, **14**(12), 5140-5147 (2002).
12. Choe, S., Lee, S. H., Chang, Y. Y., Hwang, K. Y., and Khim, J., "Rapid reductive destruction of hazardous organic compounds by nanoscale Fe-0," *Chemosphere*, **42**(4), 367-372 (2001).
13. Xu, Y. and Zhang, W. X., "Subcolloidal Fe/Ag particles for reductive dehalogenation of chlorinated benzenes," *Ind. & Eng. Chem. Res.*, **39**(7), 2238-2244 (2000).
14. Ponder, S. M., Darab, J. G., and Mallouk, T. E., "Remediation of Cr(VI) and Pb(II) aqueous solutions using supported, nanoscale zero-valent iron," *Environ. Sci. & Tech.*, **34** (12), 2564-2569 (2000).
15. Ponder, S. M., Darab, J. G., Bucher, J., Caulder, D., Craig, I., Davis, L., Edelstein, N., Lukens, W., Nitsche, H., Rao, L. F., Shuh, D. K., and Mallouk, T. E., "Surface chemistry and electrochemistry of supported zerovalent iron nanoparticles in the remediation of aqueous metal contaminants," *Chem. of Mat.*, **13**(2), 479-486 (2001).
16. Choe, S., Chang, Y. Y., Hwang, K. Y., and Khim, J., "Kinetics of reductive denitrification by nanoscale zero-valent iron," *Chemosphere*, **41**(8), 1307-1311 (2000).
17. Scherer, M. M., Balko, A. D., and Tratnyek, P. G., The role of oxides in the reduction reaction at the metal-water interface. In: Sparks, D. and Grundl, T. (eds). *Mineral-Water Interfacial Reactions:Kinetics and Mechanisms*, Americal Chemical Society, Washington, DC. pp. 301-322 (1998).
18. Kim, Y., "Reductive dechlorination of chlorinated biphenyls by palladium coated zinc, *Environ. Eng. Res.*, **7**, 239-245, 2002.
19. Song, H., Carraway, E., and Kim, Y., "Synthesis of nano-sized iron for reductive dechlorination. 2. Effects of synthesis conditions on reactivities of the iron," *Environ. Eng. Res.*, submitted 2005.
20. U.S. Environmental Protection Agency., Preparing perfect project plans. EPA-800-9-89-087 (1989).

21. Stumm, W. and Morgan, J. J., *Aquatic Chemistry,* John Wiley & Sons, Inc., New York, NY (1996).
22. Zhang, L. and Manthiram, A., "Chains composed of nanosize metal particles and identifying the factors driving their formation." *Appl. Phy. Letters,* **70**(18), 2469-2471 (1997).
23. Darroudi, T., personal communication, Electron microscope laboratory, Clemson University, October (2003).